

l_0 -norm Based Algorithm for Training Fault Tolerant RBF Networks and Selecting Centers

Hao Wang, Chi-Sing Leung, *Member, IEEE*, Hing Cheung So, *Fellow, IEEE*, Ruibin Feng, and Zifa Han

Abstract—The aim of this paper is to train an RBF neural network and select centers under concurrent faults. It is well known that fault tolerance is a very attractive property for neural networks. And center selection is an important procedure during the training process of an RBF neural network. In this paper, we devise two novel algorithms to address these two issues simultaneously. Both of them are based on the ADMM framework. In the first method, the minimax concave penalty (MCP) function is introduced to select centers. In the second method, an l_0 -norm term is directly used, and the hard threshold (HT) is utilized to address the l_0 -norm term. Under several mild conditions, we can prove that both methods can globally converge to a unique limit point. Simulation results show that, under concurrent fault, the proposed algorithms are superior to many existing methods.

Index Terms—failure tolerant, RBF, center selection, ADMM, l_0 -norm, MCP, hard threshold.

I. INTRODUCTION

Radial basis function (RBF) neural network is a common algorithm and is widely used in many applications [1]–[3]. Its training process usually includes two stages. In the first phase, the RBF centers are determined. And in the second phase, the corresponding weights of these RBF centers are estimated. These RBF centers are usually selected from the training set. For instance, we can use all input vectors from the training samples as RBF centers [4], or randomly choose a subset from the training set [5]. However, the first method may result in a complex network structure and the problem of overfitting. The second method cannot guarantee that the constructed RBF network covers the input space well.

To overcome the shortcomings of the above two methods, many other RBF center selection approaches have been proposed. Among them, clustering algorithm [6], orthogonal least squares (OLS) approach [7], [8], and support vector regression [9], [10] are the most representative methods. None of these algorithms involve situations where network faults have occurred. However, during the training process of neural networks, the network faults are almost inevitable. For example, when we calculate the centers' weights, the round-off errors will be introduced which can be seen as a kind of multiplicative weight fault [11]–[13]. When the connection between two neurons is damaged, signals cannot transform between them which may result in the open weight fault [14], [15].

Over the past two decades, several fault tolerant neural networks have been proposed. Most of them only consider

one kind of network fault [16]–[19]. However, the paper [20] first describes a situation when the multiplicative weight fault and open weight fault occur in a neural network concurrently. Due to the modification of its objective function, the solution of this method is biased. To handle this issue, a new approach based on OLS and regularization term is proposed in [21]. The performance of this algorithm is better than most existing methods. But the computational cost is very expensive, since the OLS approach is used in this method. And this method can only carry out the center selection steps before the training process. In order to further improve the performance of an RBF network and perform center selection and training at the same time, a fault tolerant RBF center selection method based on l_1 -norm is proposed in our previous work [22].

In this paper, we further develop our previous work by replacing the l_1 -norm regularization with the l_0 -norm term. And then we propose two methods to solve this problem. In the first one, we further modify the objective by introducing the minimax concave penalty (MCP) function to substitute the l_0 -norm term. After that, the problem is solved by alternating direction method of multipliers (ADMM) framework. In the second method, the ADMM framework and hard threshold (HT) are utilized to solve the problem. The main contribution of this paper is: (i). Two novel fault tolerant RBF center selection algorithms are developed. (ii). We theoretically prove that the proposed methods can globally converge to a unique limit point. (iii). The performance improvements of the proposed methods are very significant.

The rest of paper is organized as follows. The background of RBF neural network under concurrent faults and the ADMM framework are described in Section II. In Section III, the proposed two approaches are developed. In Section IV, we prove that both our proposed methods can globally converge to a unique limit point under mild conditions. Numerical results for evaluation and comparison of different algorithms are provided in Section V. Finally, the conclusions are drawn in Section VI.

II. BACKGROUND

A. Notation

We use a lower-case or upper-case letter to represent a scalar while vectors and matrices are denoted by bold lower-case and upper-case letters, respectively. The transpose operator is denoted as $(\cdot)^T$, and \mathbf{I} represents the identity matrix with appropriate dimensions. Other mathematical symbols are defined in their first appearance.

Hao Wang, Chi-Sing Leung, Hing Cheung So, Ruibin Feng, and Zifa Han are with the Department of Electronic Engineering, City University of Hong Kong Kowloon Tong, Kowloon, Hong Kong.

B. RBF networks under concurrent fault situation

In this paper, the training set is expressed as

$$\mathcal{D} = \{(\mathbf{x}_i, y_i) : \mathbf{x}_i \in \mathbb{R}^{K_1}, y_i \in \mathbb{R}, i = 1, 2, \dots, N\}, \quad (1)$$

where \mathbf{x}_i is the input of the i -th sample with dimension K_1 , and y_i is the corresponding output. Similarly, the test set can be denoted as

$$\mathcal{D}' = \{(\mathbf{x}'_{i'}, y'_{i'}) : \mathbf{x}'_{i'} \in \mathbb{R}^{K_1}, y'_{i'} \in \mathbb{R}, i' = 1, 2, \dots, N'\}. \quad (2)$$

Generally speaking, the RBF approach is used to handle regression problems. The input-output relationship of data in \mathcal{D} is approximated by the sums of M radial basis functions, i.e.,

$$f(\mathbf{x}) = \sum_{j=1}^M w_j \exp\left(\frac{-\|\mathbf{x} - \mathbf{c}_j\|_2^2}{s}\right), \quad (3)$$

where $\exp\left(\frac{-\|\mathbf{x} - \mathbf{c}_j\|_2^2}{s}\right)$ is the j -th radial basis function, w_j denotes its weight, the vectors \mathbf{c}_j 's are the RBF centers, s is a parameter which can be used to control the radial basis function width, and M denotes the number of RBF centers. Usually, the centers are selected from the input data $\{\mathbf{x}_1, \dots, \mathbf{x}_N\}$. If we directly use all inputs as centers, it may result in some ill-conditioned solutions. Therefore, center selection is a key step in RBF neural network.

For a faulty-free network, the training set error can be expressed as

$$\begin{aligned} \mathcal{E}_{train} &= \frac{1}{N} \sum_{i=1}^N (y_i - f(\mathbf{x}_i))^2 \\ &= \frac{1}{N} \sum_{i=1}^N \left(y_i - \sum_{j=1}^M w_j \exp\left(\frac{-\|\mathbf{x}_i - \mathbf{c}_j\|_2^2}{s}\right) \right)^2 \\ &= \frac{1}{N} \|\mathbf{y} - \mathbf{A}\mathbf{w}\|_2^2, \end{aligned} \quad (4)$$

where $\mathbf{w} = [w_1, \dots, w_M]^T$, $\mathbf{y} = [y_1, \dots, y_N]^T$, and \mathbf{A} is a $N \times M$ matrix. Let $a_j(\mathbf{x}_i)$ denotes the (i, j) entry of \mathbf{A} ,

$$a_j(\mathbf{x}_i) = [\mathbf{A}]_{i,j} = \exp\left(\frac{-\|\mathbf{x}_i - \mathbf{c}_j\|_2^2}{s}\right). \quad (5)$$

However, in the implementation of an RBF neural network, weight failures may happen. Multiplicative weight noise and open weight fault are two common faults in the RBF neural network [11]–[13], [16], [18], [19], [23], [24]. When they are concurrent [20], [21], the weights can be modeled as

$$\tilde{w}_j = (w_j + b_j w_j) \beta_j, \quad (6)$$

where $j = 1, \dots, M$, β_j denotes the open fault of the j th weight. When the connection is opened, $\beta_j = 0$, otherwise, $\beta_j = 1$. The term $b_j w_j$ in (6) is the multiplicative noise in j th weight. The magnitude of the noise is proportional to that of the weight. We assume that the b_j 's are independent and identically distributed (i.i.d.) zero-mean random variables with

variance σ_b^2 . With this assumption, the statistics of b_j 's are summarized as

$$\langle b_j \rangle = 0, \quad \langle b_j^2 \rangle = \sigma_b^2, \quad (7a)$$

$$\langle b_j b_{j'} \rangle = 0, \quad \forall j \neq j', \quad (7b)$$

where $\langle \cdot \rangle$ is an expectation operator. Furthermore, we assume that β_j 's are i.i.d. binary random variables. The probability mass function of β_j is given by

$$\text{Prob}(\beta_j) = \begin{cases} P_\beta, & \text{for } \beta_j = 0, \\ 1 - P_\beta, & \text{for } \beta_j = 1. \end{cases} \quad (8)$$

Thus, the statistics of β_j 's are

$$\langle \beta_j \rangle = \langle \beta_j^2 \rangle = 1 - P_\beta, \quad (10a)$$

$$\langle \beta_j \beta_{j'} \rangle = (1 - P_\beta)^2, \quad \forall j \neq j'. \quad (10b)$$

Given a particular fault pattern of b_j and β_j , the training set error can be expressed as

$$\begin{aligned} \tilde{\mathcal{E}}_{train} &= \frac{1}{N} \|\mathbf{y} - \mathbf{A}\tilde{\mathbf{w}}\|_2^2 \\ &= \frac{1}{N} \sum_{i=1}^N \left[y_i^2 - 2y_i \sum_{j=1}^M \beta_j w_j a_j(\mathbf{x}_i) \right. \\ &\quad + \sum_{j=1}^M \sum_{j'=j}^M \beta_j \beta_{j'} w_j w_{j'} (1 + b_j b_{j'}) a_j(\mathbf{x}_i) a_{j'}(\mathbf{x}_i) \\ &\quad + \sum_{j=1}^M \sum_{j'=1}^M (b_j + b_{j'}) \beta_j \beta_{j'} w_j w_{j'} a_j(\mathbf{x}_i) a_{j'}(\mathbf{x}_i) \\ &\quad \left. - 2y_i \sum_{j=1}^M b_j \beta_j w_j a_j(\mathbf{x}_i) \right]. \end{aligned} \quad (11)$$

From (7) and (10), the average training set error [21] over all possible failures is given by

$$\begin{aligned} \bar{\mathcal{E}}_{train} &= \frac{P_\beta}{N} \sum_{i=1}^N y_i^2 + \frac{1 - P_\beta}{N} \|\mathbf{y} - \mathbf{A}\mathbf{w}\|_2^2 \\ &\quad + \frac{1 - P_\beta}{N} \mathbf{w}^T [(P_\beta + \sigma_b^2) \text{diag}(\mathbf{A}^T \mathbf{A}) - P_\beta \mathbf{A}^T \mathbf{A}] \mathbf{w}. \end{aligned} \quad (12)$$

In (12), the term $\frac{P_\beta}{N} \sum_{i=1}^N y_i^2$ can be seen as a constant with respect to the weight vector \mathbf{w} . Hence the training objective function can be defined as

$$\psi(\mathbf{w}) = \frac{1}{N} \|\mathbf{y} - \mathbf{A}\mathbf{w}\|_2^2 + \mathbf{w}^T \mathbf{R} \mathbf{w}, \quad (13)$$

where $\mathbf{R} = (P_\beta + \sigma_b^2) \text{diag}\left(\frac{1}{N} \mathbf{A}^T \mathbf{A}\right) - \frac{P_\beta}{N} \mathbf{A}^T \mathbf{A}$.

C. ADMM

The ADMM framework is an iterative approach for solving optimization problems by breaking them into smaller subproblems [25]. This algorithm can be used to solve problems in the standard form

$$\min_{\mathbf{z}, \mathbf{y}} : \psi(\mathbf{z}) + g(\mathbf{y}) \quad (14a)$$

$$\text{s.t.} \quad \mathbf{C}\mathbf{z} + \mathbf{D}\mathbf{y} = \mathbf{b}. \quad (14b)$$

with variables $\mathbf{z} \in \mathbb{R}^n$ and $\mathbf{y} \in \mathbb{R}^m$, where $\mathbf{b} \in \mathbb{R}^p$, $\mathbf{C} \in \mathbb{R}^{p \times n}$ and $\mathbf{D} \in \mathbb{R}^{p \times m}$. In the ADMM framework, first we construct an augmented Lagrangian function as

$$L(\mathbf{z}, \mathbf{y}, \boldsymbol{\alpha}) = \psi(\mathbf{z}) + g(\mathbf{y}) + \boldsymbol{\alpha}^T (\mathbf{C}\mathbf{z} + \mathbf{D}\mathbf{y} - \mathbf{b}) + \frac{\rho}{2} \|\mathbf{C}\mathbf{z} + \mathbf{D}\mathbf{y} - \mathbf{b}\|_2^2, \quad (15)$$

where $\boldsymbol{\alpha} \in \mathbb{R}^p$ is the Lagrange multiplier vector, and $\rho > 0$. The algorithm consists of the iterations as:

$$\mathbf{z}^{k+1} = \underset{\mathbf{y}}{\operatorname{argmin}} L(\mathbf{z}^k, \mathbf{y}, \boldsymbol{\alpha}^k), \quad (16a)$$

$$\mathbf{y}^{k+1} = \underset{\mathbf{z}}{\operatorname{argmin}} L(\mathbf{z}, \mathbf{y}^{k+1}, \boldsymbol{\alpha}^k), \quad (16b)$$

$$\boldsymbol{\alpha}^{k+1} = \boldsymbol{\alpha}^k + \rho (\mathbf{C}\mathbf{z}^{k+1} + \mathbf{D}\mathbf{y}^{k+1} - \mathbf{b}). \quad (16c)$$

For updating the dual variable, a step size equal to the augmented Lagrangian parameter ρ is used.

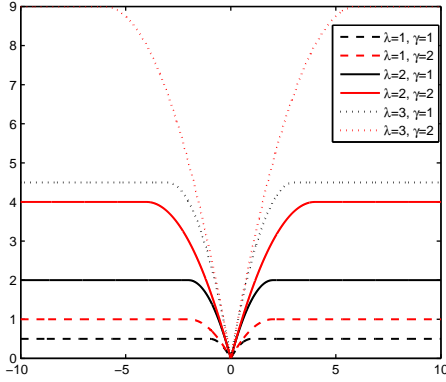


Fig. 1: The shapes of MCP penalty function under different parameter settings.

III. DEVELOPMENT OF PROPOSED ALGORITHM

In (13), we use M RBF centers. To limit the size of the RBF network and automatically select appropriate centers during training process, we further modify the objective function and propose two novel algorithms based on the property of l_0 -norm and ADMM framework.

A. RBF center selection based on ADMM-MCP

In the first method, we consider introducing an additional penalty term $\lambda \|\mathbf{w}\|_0$ into (13), then we have

$$\hat{Q}(\mathbf{w}, \lambda) = \frac{1}{N} \|\mathbf{y} - \mathbf{A}\mathbf{w}\|_2^2 + \mathbf{w}^T \mathbf{R}\mathbf{w} + \lambda \|\mathbf{w}\|_0, \quad (17)$$

where $\|\mathbf{w}\|_0$ represents the number of non-zero entries in \mathbf{w} . Due to the nature of l_0 -norm, the problem in (17) is NP hard [26]. To handle this issue, the MCP function is introduced, which is a very attractive approximate function of l_0 -norm [27], [28]. Thus, the function in (17) can be rewritten as

$$Q(\mathbf{w}, \lambda) = \frac{1}{N} \|\mathbf{y} - \mathbf{A}\mathbf{w}\|_2^2 + \mathbf{w}^T \mathbf{R}\mathbf{w} + P_{\lambda, \gamma}(\mathbf{w}), \quad (18)$$

where $P_{\lambda, \gamma}(\mathbf{w}) = \sum_{i=1}^M P_{\lambda, \gamma}(w_i)$ ($\lambda > 0, \gamma > 0$) denotes the MCP function,

$$P_{\lambda, \gamma}(w_i) = \begin{cases} \lambda |w_i| - \frac{w_i^2}{2\gamma}, & \text{if } |w_i| \leq \gamma\lambda, \\ \frac{1}{2}\gamma\lambda^2, & \text{if } |w_i| > \gamma\lambda. \end{cases} \quad (19)$$

and

$$\begin{aligned} \frac{\partial P_{\lambda, \gamma}(\mathbf{w})}{\partial w_i} &= \lambda \operatorname{sign}(w_i) \left(1 - \frac{|w_i|}{\lambda\gamma}\right)_+ \\ &= \begin{cases} \lambda \operatorname{sign}(w_i) - \frac{w_i}{\gamma}, & \text{if } |w_i| \leq \gamma\lambda, \\ 0, & \text{if } |w_i| > \gamma\lambda. \end{cases} \end{aligned} \quad (20)$$

The shapes of MCP penalty function with different parameter settings are shown in Fig. 1. From this figure, we see that, with appropriate parameter setting, the shape of MCP is very similar with the l_0 -norm term.

Then the ADMM framework is used to handle the problem in (18). Following the steps of ADMM, we introduce a dummy variable $\mathbf{u} = [u_1, \dots, u_M]^T$ and transform the unconstrained problem into the standard constrained form

$$\min_{\mathbf{w}, \mathbf{u}} \psi(\mathbf{w}) + P_{\lambda, \gamma}(\mathbf{u}), \quad (21a)$$

$$\text{s.t. } \mathbf{u} = \mathbf{w}, \quad (21b)$$

where $\psi(\mathbf{w})$ is given by (13). Then we construct its augmented Lagrangian as

$$L(\mathbf{w}, \mathbf{u}, \mathbf{v}) = \psi(\mathbf{w}) + P_{\lambda, \gamma}(\mathbf{u}) + \mathbf{v}^T (\mathbf{u} - \mathbf{w}) + \frac{\rho}{2} \|\mathbf{w} - \mathbf{u}\|_2^2, \quad (22)$$

According to (16), the ADMM iteration of \mathbf{u}^{k+1} is

$$\begin{aligned} \mathbf{u}^{k+1} &= \underset{\mathbf{u}}{\operatorname{argmin}} L(\mathbf{w}^k, \mathbf{u}, \mathbf{v}^k), \\ &= \underset{\mathbf{u}}{\operatorname{argmin}} P_{\lambda, \gamma}(\mathbf{u}) + \mathbf{v}^{kT} (\mathbf{u} - \mathbf{w}^k) + \frac{\rho}{2} \|\mathbf{w}^k - \mathbf{u}\|_2^2 \\ &= \underset{\mathbf{u}}{\operatorname{argmin}} P_{\lambda, \gamma}(\mathbf{u}) + \frac{\rho}{2} \left\| \mathbf{w}^k - \mathbf{u} - \frac{1}{\rho} \mathbf{v}^k \right\|_2^2 \end{aligned} \quad (23)$$

where $\mathbf{u}^{k+1} = [u_1^{k+1}, \dots, u_M^{k+1}]^T$. For any u_i ($i \in [1, \dots, M]$), if $\rho > \frac{1}{\gamma}$ then

$$u_i^{k+1} = \begin{cases} \frac{S(w_i^k - v_i^k/\rho, \frac{\lambda}{\rho})}{1 - 1/(\gamma\rho)}, & \text{if } |w_i^k - v_i^k/\rho| \leq \gamma\lambda, \\ w_i^k - v_i^k/\rho, & \text{if } |w_i^k - v_i^k/\rho| > \gamma\lambda, \end{cases} \quad (24)$$

where S denotes the soft-threshold operator [29] given by

$$S(z, \eta) = \operatorname{sign}(z) \max\{|z| - \eta, 0\},$$

if $\rho = \frac{1}{\gamma}$,

$$u_i^{k+1} = \begin{cases} 0, & \text{if } |w_i^k - v_i^k/\rho| \leq \gamma\lambda, \\ w_i^k - v_i^k/\rho, & \text{if } |w_i^k - v_i^k/\rho| > \gamma\lambda, \end{cases} \quad (25)$$

if $\rho < \frac{1}{\gamma}$,

$$u_i^{k+1} = \begin{cases} 0, & \text{if } |w_i^k - v_i^k/\rho| \leq \sqrt{\frac{2}{\rho}}\lambda, \\ w_i^k - v_i^k/\rho, & \text{if } |w_i^k - v_i^k/\rho| > \sqrt{\frac{2}{\rho}}\lambda. \end{cases} \quad (26)$$

All these three cases have a unified approximate solution [27], [28]

$$u_i^{k+1} = \begin{cases} \frac{S(w_i^k - v_i^k/\rho, \lambda)}{1 - 1/\gamma}, & \text{if } |w_i^k - v_i^k/\rho| \leq \gamma\lambda, \\ w_i^k - v_i^k/\rho, & \text{if } |w_i^k - v_i^k/\rho| > \gamma\lambda. \end{cases} \quad (27)$$

It is worth noting that when $\gamma \rightarrow \infty$ the function in (27) is similar with the soft-threshold, when $\gamma \rightarrow 1$ the function is close to the hard-threshold.

\mathbf{w}^{k+1} is directly calculated by first-order optimization condition, the solution is given by

$$\begin{aligned} \mathbf{w}^{k+1} &= \underset{\mathbf{w}}{\operatorname{argmin}} L(\mathbf{w}, \mathbf{u}^{k+1}, \mathbf{v}^k) \\ &= \underset{\mathbf{w}}{\operatorname{argmin}} \psi(\mathbf{w}) + \mathbf{v}^{k\top}(\mathbf{u}^{k+1} - \mathbf{w}) + \frac{\rho}{2} \|\mathbf{w} - \mathbf{u}^{k+1}\|_2^2 \\ &= \underset{\mathbf{w}}{\operatorname{argmin}} \psi(\mathbf{w}) + \frac{\rho}{2} \left\| \mathbf{w} - \mathbf{u}^{k+1} - \frac{1}{\rho} \mathbf{v}^k \right\|_2^2 \\ &= \left[\frac{2}{N} \mathbf{A}^\top \mathbf{A} + 2\mathbf{R} + \rho \mathbf{I} \right]^{-1} \left[\frac{2}{N} \mathbf{A}^\top \mathbf{y} + \rho \mathbf{u}^{k+1} + \mathbf{v}^k \right], \end{aligned} \quad (28)$$

\mathbf{v}^{k+1} is updated as

$$\mathbf{v}^{k+1} = \mathbf{v}^k + \rho (\mathbf{u}^{k+1} - \mathbf{w}^{k+1}). \quad (29)$$

B. RBF center selection based on ADMM-HT

In the first method, two parameters λ and γ are used. If we need the number of centers exactly equal to a certain value, we have to regularize λ to meet this requirement. It is very inconvenient. Hence we propose the second method which can directly limit the maximum number of centers. First, the problem in (13) is modified as a constrained form

$$\underset{\mathbf{w}}{\operatorname{argmin}} \frac{1}{N} \|\mathbf{y} - \mathbf{A}\mathbf{w}\|_2^2 + \mathbf{w}^\top \mathbf{R}\mathbf{w}, \quad (30a)$$

$$\text{s.t.} \quad \|\mathbf{w}\|_0 \leq K. \quad (30b)$$

With the constraint in (30b), we can ensure that the number of RBF centers is equal to or smaller than K . But this problem cannot be directly solved by the ADMM framework. Since the constraint in (30b) is undecomposable. To solve this issue, we introduce an indicator function

$$i_{\mathbf{c}(K)}(\mathbf{w}) = \begin{cases} 0, & \text{if } \mathbf{w} \in \mathbf{c}(K), \\ +\infty, & \text{otherwise,} \end{cases} \quad (31)$$

where the set $\mathbf{c}(K) = \{\mathbf{w} : \|\mathbf{w}\|_0 \leq K\}$ ($K \leq M$). After that, the problem in (30) can be rewritten as

$$\underset{\mathbf{w}}{\operatorname{argmin}} \frac{1}{N} \|\mathbf{y} - \mathbf{A}\mathbf{w}\|_2^2 + \mathbf{w}^\top \mathbf{R}\mathbf{w} + i_{\mathbf{c}(K)}(\mathbf{w}). \quad (32)$$

Then, we introduce a dummy variable \mathbf{u} and rewrite problem in (32) as

$$\underset{\mathbf{w}}{\operatorname{argmin}} \psi(\mathbf{w}) + g(\mathbf{u}), \quad (33a)$$

$$\text{s.t.} \quad \mathbf{w} = \mathbf{u}, \quad (33b)$$

where $g(\mathbf{u})$ denotes the indicator function $i_{\mathbf{c}(K)}(\mathbf{u})$. Its augmented Lagrangian is

$$\begin{aligned} L(\mathbf{w}, \mathbf{u}, \mathbf{v}) &= \psi(\mathbf{w}) + g(\mathbf{u}) + \mathbf{v}^\top (\mathbf{u} - \mathbf{w}) \\ &\quad + \frac{\rho}{2} \|\mathbf{w} - \mathbf{u}\|_2^2, \end{aligned} \quad (34)$$

According to (34) and (16), we have:

$$\begin{aligned} \mathbf{u}^{k+1} &= \underset{\mathbf{u}}{\operatorname{argmin}} L(\mathbf{w}^k, \mathbf{u}, \mathbf{v}^k), \\ &= \underset{\mathbf{u}}{\operatorname{argmin}} g(\mathbf{u}) + \frac{\rho}{2} \left\| \mathbf{w}^k - \mathbf{u} - \frac{1}{\rho} \mathbf{v}^k \right\|_2^2, \\ &= HT(\mathbf{w}^k - \mathbf{v}^k / \rho), \end{aligned} \quad (35)$$

where $HT(\mathbf{z})$ sets all elements of \mathbf{z} equal to 0 except the K entries with the largest magnitudes. Obviously, the HT operation can restrict \mathbf{u} into the feasible region $\mathbf{c}(K)$. It is worth noting that the second method just replaces the MCP function in the Lagrangian (22) by the indicator function $i_{\mathbf{c}(K)}(\mathbf{u})$. It does not influence the update of \mathbf{w}^{k+1} and \mathbf{v}^{k+1} . Hence in the second method we still have:

$$\mathbf{w}^{k+1} = \left[\frac{2}{N} \mathbf{A}^\top \mathbf{A} + 2\mathbf{R} + \rho \mathbf{I} \right]^{-1} \left[\frac{2}{N} \mathbf{A}^\top \mathbf{y} + \rho \mathbf{u}^{k+1} + \mathbf{v}^k \right]. \quad (36)$$

and

$$\mathbf{v}^{k+1} = \mathbf{v}^k + \rho (\mathbf{u}^{k+1} - \mathbf{w}^{k+1}). \quad (37)$$

IV. ANALYSIS OF GLOBAL CONVERGENCE

In this section, we discuss the convergence of the proposed methods. We cannot directly follow the general convergence proof for nonconvex ADMM given by [30]. Because some of the assumptions given in [30] are not satisfied. For instance, $i_{\mathbf{c}(K)}(\mathbf{u})$ is not a restricted prox-regular function. But the global convergence of our proposed two methods still can be proved. We first give a sketch of the proof in Theorem 1, and the details are discussed latter.

Theorem 1: If the proposed methods satisfy the following four conditions:

C1 (Sufficient decrease condition) For each k , $\exists \tau_1 > 0$ let

$$L(\mathbf{w}^{k+1}, \mathbf{u}^{k+1}, \mathbf{v}^{k+1}) - L(\mathbf{w}^k, \mathbf{u}^k, \mathbf{v}^k) \leq -\tau_1 \|\mathbf{w}^{k+1} - \mathbf{w}^k\|_2^2. \quad (38)$$

C2 (Boundness condition) The sequences $\{\mathbf{w}^k, \mathbf{u}^k, \mathbf{v}^k\}$ generated by the proposed two methods are bounded and their Lagrangian functions are lower bounded.

C3 (Subgradient bound condition) For each $k \in \mathbb{N}$, there exists a $\mathbf{d}^{k+1} \in \partial L(\mathbf{w}^{k+1}, \mathbf{u}^{k+1}, \mathbf{v}^{k+1})$, and a $\tau_2 > 0$ such that

$$\|\mathbf{d}^{k+1}\|_2^2 \leq \tau_2 \|\mathbf{w}^{k+1} - \mathbf{w}^k\|_2^2. \quad (39)$$

C4 (Continuity condition) If $\{\mathbf{w}^*, \mathbf{u}^*, \mathbf{v}^*\}$ is the limit point of a sub-sequence $\{\mathbf{w}^{k_s}, \mathbf{u}^{k_s}, \mathbf{v}^{k_s}\}$ ($s \in \mathbb{N}$), then $L(\mathbf{w}^*, \mathbf{u}^*, \mathbf{v}^*) = \lim_{s \rightarrow \infty} L(\mathbf{w}^{k_s}, \mathbf{u}^{k_s}, \mathbf{v}^{k_s})$.

Based on these conditions, we can further deduce that the sequences $\{\mathbf{w}^k, \mathbf{u}^k, \mathbf{v}^k\}$ have at least one limit point $\{\mathbf{w}^*, \mathbf{u}^*, \mathbf{v}^*\}$ and any limit point $\{\mathbf{w}^*, \mathbf{u}^*, \mathbf{v}^*\}$ is a stationary point. Moreover, if their Lagrangian functions $L(\mathbf{w}, \mathbf{u}, \mathbf{v})$ are Kurdyka-Łojasiewicz (KL) function, then the sequences $\{\mathbf{w}^k, \mathbf{u}^k, \mathbf{v}^k\}$ will globally converge to a unique limit point $\{\mathbf{w}^*, \mathbf{u}^*, \mathbf{v}^*\}$.

Proof: The theorem is similar as Proposition 2 in [30] and Theorem 2.9 in [31]. The proof of it is also standard. So we omit it here. The details can be found in the proof of Proposition 2 in [30]. ■

For the proof of convergence, the key step here is to prove that the above mentioned four conditions are satisfied. Hence, we have the following four propositions.

Proposition 1: If ρ is greater than a certain value, the proposed two methods satisfy the sufficient decrease condition in C1.

Proof: In the following proof, we use the second method as an example. For the first method, the proof is same except replacing the function $g(\mathbf{u})$ by $P_{\lambda, \gamma}(\mathbf{u})$.

For the second method, the Lagrangian function in (34) can be rewritten as

$$L(\mathbf{w}, \mathbf{u}, \mathbf{v}) = \psi(\mathbf{w}) + \frac{\rho}{2} \left\| \mathbf{w} - \mathbf{u} - \frac{1}{\rho} \mathbf{v} \right\|_2^2 + g(\mathbf{u}) - \frac{1}{2\rho} \|\mathbf{v}\|_2^2. \quad (40)$$

The second-order derivative of $\psi(\mathbf{w})$ is

$$\begin{aligned} \frac{\partial^2 \psi(\mathbf{w})}{\partial \mathbf{w}^2} &= \frac{2}{N} \mathbf{A}^T \mathbf{A} + 2\mathbf{R} \\ &= \frac{2}{N} [(1 - P_\beta) \mathbf{A}^T \mathbf{A} + (P_\beta + \sigma_b^2) \text{diag}(\mathbf{A}^T \mathbf{A})]. \end{aligned} \quad (41)$$

Obviously, it is positive definite. Hence $\psi(\mathbf{w})$ is strongly convex. We can further deduce that the Lagrangian in (40) is also strongly convex with respect to \mathbf{w} . Hence, based on the definition of strongly convex function, we have

$$\begin{aligned} L(\mathbf{w}^{k+1}, \mathbf{u}^{k+1}, \mathbf{v}^k) - L(\mathbf{w}^k, \mathbf{u}^{k+1}, \mathbf{v}^k) \\ \leq -\frac{a}{2} \|\mathbf{w}^{k+1} - \mathbf{w}^k\|_2^2, \end{aligned} \quad (42)$$

where $a > 0$.

From (36), we have

$$\nabla \psi(\mathbf{w}^{k+1}) - \mathbf{v}^k + \rho(\mathbf{w}^{k+1} - \mathbf{u}^{k+1}) = 0. \quad (43)$$

Combining it with (37), we can deduce that $\nabla \psi(\mathbf{w}^{k+1}) = \mathbf{v}^{k+1}$ and $\mathbf{u}^{k+1} - \mathbf{w}^{k+1} = 1/\rho (\mathbf{v}^{k+1} - \mathbf{v}^k)$. Thus

$$\begin{aligned} &L(\mathbf{w}^{k+1}, \mathbf{u}^{k+1}, \mathbf{v}^{k+1}) - L(\mathbf{w}^{k+1}, \mathbf{u}^{k+1}, \mathbf{v}^k) \\ &= (\mathbf{v}^{k+1} - \mathbf{v}^k)^T (\mathbf{u}^{k+1} - \mathbf{w}^{k+1}) \\ &= \frac{1}{\rho} \|\mathbf{v}^{k+1} - \mathbf{v}^k\|_2^2 = \frac{1}{\rho} \|\nabla \psi(\mathbf{w}^{k+1}) - \nabla \psi(\mathbf{w}^k)\|_2^2 \\ &\leq \frac{l_\psi^2}{\rho} \|\mathbf{w}^{k+1} - \mathbf{w}^k\|_2^2, \end{aligned} \quad (44)$$

where l_ψ is a Lipschitz constant of function $\psi(\mathbf{w})$. The last inequality in (44) is because that $\psi(\mathbf{w})$ has Lipschitz continuous gradient.

From (35), we have

$$L(\mathbf{w}^k, \mathbf{u}^{k+1}, \mathbf{v}^k) - L(\mathbf{w}^k, \mathbf{u}^k, \mathbf{v}^k) \leq 0 \quad (45)$$

Combining (42), (44) and (45), we have

$$\begin{aligned} &L(\mathbf{w}^{k+1}, \mathbf{u}^{k+1}, \mathbf{v}^{k+1}) - L(\mathbf{w}^k, \mathbf{u}^k, \mathbf{v}^k) \\ &= L(\mathbf{w}^{k+1}, \mathbf{u}^{k+1}, \mathbf{v}^{k+1}) - L(\mathbf{w}^{k+1}, \mathbf{u}^{k+1}, \mathbf{v}^k) \\ &\quad + L(\mathbf{w}^{k+1}, \mathbf{u}^{k+1}, \mathbf{v}^k) - L(\mathbf{w}^k, \mathbf{u}^{k+1}, \mathbf{v}^k) \\ &\quad + L(\mathbf{w}^k, \mathbf{u}^{k+1}, \mathbf{v}^k) - L(\mathbf{w}^k, \mathbf{u}^k, \mathbf{v}^k) \\ &\leq \left(\frac{l_\psi^2}{\rho} - \frac{a}{2} \right) \|\mathbf{w}^{k+1} - \mathbf{w}^k\|_2^2. \end{aligned} \quad (46)$$

If $\rho > 2l_\psi^2/a$, we can ensure that $l_\psi^2/\rho - a/2 < 0$. Hence the $\tau_1 = a/2 - l_\psi^2/\rho$ in **C1**. ■

Proposition 2: If $\rho \geq l_\psi$, $L(\mathbf{w}^k, \mathbf{u}^k, \mathbf{v}^k)$ is lower bounded, and the sequences $\{\mathbf{w}^k, \mathbf{u}^k, \mathbf{v}^k\}$ generated by the proposed methods are bounded.

Proof: We still use the second method as an example. The proof of the first method is also similar. Firstly, we prove the $L(\mathbf{w}^k, \mathbf{u}^k, \mathbf{v}^k)$ is lower bounded for all k .

$$\begin{aligned} L(\mathbf{w}^k, \mathbf{u}^k, \mathbf{v}^k) &= \psi(\mathbf{w}^k) + g(\mathbf{u}^k) + \mathbf{v}^k{}^T (\mathbf{u}^k - \mathbf{w}^k) \\ &\quad + \frac{\rho}{2} \|\mathbf{w}^k - \mathbf{u}^k\|_2^2, \\ &= \psi(\mathbf{w}^k) + g(\mathbf{u}^k) + \nabla \psi(\mathbf{w}^k)^T (\mathbf{u}^k - \mathbf{w}^k) \\ &\quad + \frac{\rho}{2} \|\mathbf{w}^k - \mathbf{u}^k\|_2^2, \\ &\geq \psi(\mathbf{u}^k) + \left(\frac{\rho}{2} - \frac{l_\psi}{2} \right) \|\mathbf{u}^k - \mathbf{w}^k\|_2^2 + g(\mathbf{u}^k), \end{aligned} \quad (47)$$

where the inequality in (47) is due to Lemma 3.1 in [31] and the Lipschitz continue gradient of $\psi(\mathbf{w})$. According to Lemma 3.1 in [31], we can deduce that

$$\psi(\mathbf{w}^k) + \nabla \psi(\mathbf{w}^k)^T (\mathbf{u}^k - \mathbf{w}^k) \geq \psi(\mathbf{u}^k) - \frac{l_\psi}{2} \|\mathbf{u}^k - \mathbf{w}^k\|_2^2,$$

thus we have the inequality in (47).

Obviously, if $\rho \geq l_\psi$, then $\psi(\mathbf{u}^k) + \left(\frac{\rho}{2} - \frac{l_\psi}{2} \right) \|\mathbf{u}^k - \mathbf{w}^k\|_2^2 + g(\mathbf{u}^k) > -\infty$ and $L(\mathbf{w}^k, \mathbf{u}^k, \mathbf{v}^k)$ is lower bounded. According to the proof of Property 1, we know $L(\mathbf{w}^k, \mathbf{u}^k, \mathbf{v}^k)$ is sufficient descent. Hence $L(\mathbf{w}^k, \mathbf{u}^k, \mathbf{v}^k)$ is upper bounded by $L(\mathbf{w}^0, \mathbf{u}^0, \mathbf{v}^0)$.

Next, we prove the sequence $\{\mathbf{w}^k, \mathbf{u}^k, \mathbf{v}^k\}$ is bounded. From inequation (46), we have

$$\begin{aligned} &\|\mathbf{w}^{k+1} - \mathbf{w}^k\|_2^2 \\ &\leq \frac{1}{\tau_1} (L(\mathbf{w}^k, \mathbf{u}^k, \mathbf{v}^k) - L(\mathbf{w}^{k+1}, \mathbf{u}^{k+1}, \mathbf{v}^{k+1})). \end{aligned}$$

Then, we can deduce that

$$\begin{aligned} &\sum_{k=1}^l \|\mathbf{w}^{k+1} - \mathbf{w}^k\|_2^2 \\ &\leq \frac{1}{\tau_1} (L(\mathbf{w}^0, \mathbf{u}^0, \mathbf{v}^0) - L(\mathbf{w}^{l+1}, \mathbf{u}^{l+1}, \mathbf{v}^{l+1})) \\ &< \infty. \end{aligned} \quad (48)$$

If $l \rightarrow \infty$, we still have $\sum_{k=1}^{\infty} \|\mathbf{w}^{k+1} - \mathbf{w}^k\|_2^2 < \infty$. Thus \mathbf{w}^k is bounded.

From (44), we know

$$\|\mathbf{v}^{k+1} - \mathbf{v}^k\|_2^2 \leq l_\psi^2 \|\mathbf{w}^{k+1} - \mathbf{w}^k\|_2^2.$$

Therefore we can also deduce that

$$\sum_{i=1}^{\infty} \|\mathbf{v}^{i+1} - \mathbf{v}^i\|_2^2 < \infty. \quad (49)$$

In addition, according to (37), we have

$$\begin{aligned} &\|\mathbf{u}^{k+1} - \mathbf{u}^k\|_2^2 \\ &= \|\mathbf{w}^{k+1} - \mathbf{w}^k + \frac{1}{\rho} (\mathbf{v}^{k+1} - \mathbf{v}^k) + \frac{1}{\rho} (\mathbf{v}^{k-1} - \mathbf{v}^k)\|_2^2 \\ &\leq 2\|\mathbf{w}^{k+1} - \mathbf{w}^k\|_2^2 + \frac{2}{\rho^2} \|\mathbf{v}^{k+1} - \mathbf{v}^k\|_2^2 \\ &\quad + \frac{2}{\rho^2} \|\mathbf{v}^{k-1} - \mathbf{v}^k\|_2^2. \end{aligned} \quad (50)$$

Thus

$$\sum_{i=1}^{\infty} \|\mathbf{u}^{k+1} - \mathbf{u}^k\|_2^2 < \infty. \quad (51)$$

So the sequence $\{\mathbf{w}^k, \mathbf{u}^k, \mathbf{v}^k\}$ is bounded. ■

Proposition 3: The proposed two methods satisfy the sub-gradient bound condition given by C3.

Proof: For the second method,

$$\begin{aligned} & \left. \frac{\partial L}{\partial \mathbf{w}} \right|_{(\mathbf{w}^{k+1}, \mathbf{u}^{k+1}, \mathbf{v}^{k+1})} \\ &= \nabla \psi(\mathbf{w}^{k+1}) + \rho (\mathbf{w}^{k+1} - \mathbf{u}^{k+1}) - \mathbf{v}^{k+1} \\ &= \mathbf{v}^k - \mathbf{v}^{k+1}, \end{aligned} \quad (52)$$

$$\begin{aligned} & \left. \frac{\partial L}{\partial \mathbf{u}} \right|_{(\mathbf{w}^{k+1}, \mathbf{u}^{k+1}, \mathbf{v}^{k+1})} \\ &= \partial g(\mathbf{u}^{k+1}) - \rho (\mathbf{w}^{k+1} - \mathbf{u}^{k+1}) + \mathbf{v}^{k+1} \\ &\supseteq \rho (\mathbf{w}^k - \mathbf{w}^{k+1}) + \mathbf{v}^{k+1} - \mathbf{v}^k, \end{aligned} \quad (53)$$

$$\begin{aligned} & \left. \frac{\partial L}{\partial \mathbf{v}} \right|_{(\mathbf{w}^{k+1}, \mathbf{u}^{k+1}, \mathbf{v}^{k+1})} \\ &= \mathbf{u}^{k+1} - \mathbf{w}^{k+1} = \frac{1}{\rho} (\mathbf{v}^{k+1} - \mathbf{v}^k), \end{aligned} \quad (54)$$

where the second equality in (53) is according to (35),

$$0 \in \partial g(\mathbf{u}^{k+1}) + \mathbf{v}^k - \rho (\mathbf{w}^k - \mathbf{u}^{k+1}), \quad (55)$$

where ∂ is a generalized notion called limiting-subdifferential [31]. Being given $\mathbf{u}^{k+1} \in \mathbf{c}(K)$, the limiting-subdifferential of $g(\mathbf{u})$ at \mathbf{u}^{k+1} is called the normal cone to $\mathbf{c}(K)$ at \mathbf{u}^{k+1} , which is denoted by $N_{\mathbf{c}}(\mathbf{u}^{k+1})$ (for $\mathbf{u}^{k+1} \notin \mathbf{c}(K)$ we set $N_{\mathbf{c}}(\mathbf{u}^{k+1}) = \emptyset$) [31]. Thus

$$\begin{aligned} \mathbf{d}^{k+1} &:= \begin{bmatrix} \mathbf{v}^k - \mathbf{v}^{k+1} \\ \rho (\mathbf{w}^k - \mathbf{w}^{k+1}) + \mathbf{v}^{k+1} - \mathbf{v}^k \\ \frac{1}{\rho} (\mathbf{v}^{k+1} - \mathbf{v}^k) \end{bmatrix} \\ &\in \partial L(\mathbf{w}^{k+1}, \mathbf{u}^{k+1}, \mathbf{v}^{k+1}) \end{aligned} \quad (56)$$

Combining it with the inequality in (44), we can deduce that

$$\|\mathbf{d}^{k+1}\|_2^2 \leq \tau_2 \|\mathbf{w}^{k+1} - \mathbf{w}^k\|_2^2. \quad (57)$$

Apparently, for the first method, we just need to replace the function $g(\mathbf{u})$ by $P_{\lambda, \gamma}(\mathbf{u})$, then all other proof is same with the above mentioned process. ■

Then, for proving the condition in C4, the following lemma is introduced.

Lemma 1: The indicator function in (31) is low semi-continuous.

Proof: From [32], we know that suppose \mathbf{X} is a topological space, a function $f : \mathbf{X} \rightarrow \mathbb{R} \cup \{-\infty, \infty\}$ is lower semi-continuous if and only if all of its lower levelsets $\{\mathbf{x} \in \mathbf{X} : f(\mathbf{x}) \leq \alpha\}$ are closed for every α .

According to this property, to prove Lemma 1, we just need to prove that for every α , the set $g(\mathbf{u}) \leq \alpha$ is closed. Obviously, the set is \emptyset or $\mathbf{c}(K)$ for $\forall \alpha$. Hence if $\mathbf{c}(K) = \{\mathbf{u} : \|\mathbf{u}\|_0 \leq K\}$ is closed, then $g(\mathbf{u})$ is a lower semi-continuous function.

Then, we prove that $\mathbf{c}(K) = \{\mathbf{u} : \|\mathbf{u}\|_0 \leq K\}$ ($K \leq M$) is a closed set. In other words, we need to prove that its

complementary set $\mathbf{c}^c(K) = \{\mathbf{u} : \|\mathbf{u}\|_0 > K\}$ ($K \leq M$) is an open set. According to the definition of open set, for $\forall \mathbf{u} \in \mathbf{c}^c(K)$, \mathbf{x} is an arbitrary variable in the neighbourhood of \mathbf{u} where $\|\mathbf{x} - \mathbf{u}\| < \epsilon$ ($\epsilon > 0$). If ϵ is small enough then $\mathbf{x} \in \mathbf{c}^c(K)$. Hence the set $\mathbf{c}^c(K) = \{\mathbf{u} : \|\mathbf{u}\|_0 > K\}$ is open, and the set $\mathbf{c}(K) = \{\mathbf{u} : \|\mathbf{u}\|_0 \leq K\}$ ($K \leq M$) is closed. Further more, $g(\mathbf{u})$ is lower semi-continuous. ■

Proposition 4: The proposed two methods satisfy the continuity condition in C4.

Proof: If the Lagrangian functions of our proposed methods are lower semi-continuous, the continuity condition in C4 is satisfied [30], [31]. For the first method, the Lagrangian function is continuous. Thus, it must be a lower semi-continuous function. For the second method, based on Lemma 1, we know that the indicator function $g(\mathbf{u})$ is lower semi-continuous. Besides, the terms $\psi(\mathbf{w})$, $\mathbf{v}^T(\mathbf{u} - \mathbf{w})$ and $\tilde{\rho}/2 \|\mathbf{w} - \mathbf{u}\|_2^2$ are all continuous function. Then we can deduce that its Lagrangian function is lower semi-continuous. The condition in C4 is satisfied. ■

Thus, based on C1-C4 in Theorem 1, we know that the sequences $\{\mathbf{w}^k, \mathbf{u}^k, \mathbf{v}^k\}$ generated by the first method and second method both have at least one limit point $\{\mathbf{w}^*, \mathbf{u}^*, \mathbf{v}^*\}$ and any limit point $\{\mathbf{w}^*, \mathbf{u}^*, \mathbf{v}^*\}$ is a stationary point. Finally, to ensure that both of them have global convergence to a unique limit point, we need to prove that their Lagrangian functions are KL function. Before that, in order to facilitate the following explanation, we introduce several fundamental definitions.

For a function $f : \mathbb{R}^n \rightarrow \mathbb{R}$, $\text{dom } f$ denotes the domain of f . A function f is proper means that $\text{dom } f \neq \emptyset$ and it can never attain $-\infty$.

A subset S of \mathbb{R}^d is a real semi-algebraic set if there exists a finite number of real polynomial functions $l_{ij}, h_{ij} : \mathbb{R}^d \rightarrow \mathbb{R}$ such that

$$S = \bigcup_{j=1}^{q_1} \bigcap_{i=1}^{q_2} \{\mathbf{z} \in \mathbb{R}^d : l_{ij}(\mathbf{z}) = 0, h_{ij}(\mathbf{z}) < 0\}.$$

A function $h : \mathbb{R}^d \rightarrow (-\infty, \infty]$ is semi-algebraic if its graph

$$\{(\mathbf{z}, t) \in \mathbb{R}^{d+1} : h(\mathbf{z}) = t\} \quad (58)$$

is a semi-algebraic set in \mathbb{R}^{d+1} .

The definition of KL function is given by [31]. Here we use Lemma 2 to prove that a function is KL function.

Lemma 2: Let $f : \mathbb{R}^n \rightarrow (-\infty, \infty]$ be a proper and lower semi-continuous function. If f is semi-algebraic, then it satisfies the KL property at any point of $\text{dom } f$. In other words, f is a KL function.

Proof: The proof of Lemma 2 is given by [33]. ■

Then, based on Lemma 2, we prove $L(\mathbf{w}^k, \mathbf{u}^k, \mathbf{v}^k)$ is a KL function. Obviously, for each proposed method, the $L(\mathbf{w}^k, \mathbf{u}^k, \mathbf{v}^k)$ is a proper and lower semi-continuous function. The key is to prove that $L(\mathbf{w}^k, \mathbf{u}^k, \mathbf{v}^k)$ is semi-algebraic. All other terms are obvious, except $P_{\lambda, \gamma}(\mathbf{u})$ in the first method and $g(\mathbf{u})$ in the second method. From [34], we know that the MCP function $P_{\lambda, \gamma}(\mathbf{u})$ is a semi-algebraic function.

For $g(\mathbf{u})$, according to the definition of semi-algebraic function, we need to prove that its graph $\{(\mathbf{u}, t) \in \mathbb{R}^{M+1} :$

Dataset	Number of features	Size of training set	Size of test set	RBF width
Abalon	7	2000	2177	0.1
Airfoil Self-Noise	5	751	752	0.5
Boston Housing	13	400	106	2
Concrete	9	500	530	0.5
Energy Efficiency	7	600	168	0.5
Wine Quality (white)	12	2000	2898	1

TABLE I: Properties of six data sets.

$g(\mathbf{u}) = t$ is a semi-algebraic subset of \mathbb{R}^{M+1} . If $t \neq 0$, the set $\{g(\mathbf{u}) = t\}$ is empty. Hence, the graph $\{(\mathbf{u}, t) \in \mathbb{R}^{M+1} : g(\mathbf{u}) = t\}$ is equal to $\{\mathbf{u} \in \mathbb{R}^M : g(\mathbf{u}) = 0\}$ which can be rewritten as $\mathbf{c}(K) = \{\mathbf{u} : \|\mathbf{u}\|_0 \leq K\} = \bigcup_{k=1}^K \{\mathbf{u} : \|\mathbf{u}\|_0 = k\}$. We know that a semi-algebraic set is stable under finite union operation. For $\forall k \leq K$, $\{\mathbf{u} : \|\mathbf{u}\|_0 = k\} = \{\mathbf{u} = [u_1, \dots, u_M]^T : \sum_{i=1}^M u_i^0 = k\}$ is semi-algebraic. Therefore $\mathbf{c}(K)$ is a semi-algebraic set, and $g(\mathbf{u})$ and $L(\mathbf{w}^k, \mathbf{u}^k, \mathbf{v}^k)$ are semi-algebraic functions. Further, $L(\mathbf{w}^k, \mathbf{u}^k, \mathbf{v}^k)$ is a KŁ function for the proposed two methods.

In summary, as long as $\tilde{\rho} > \max\{2\hat{l}_\psi^2/\hat{\alpha}, \hat{l}_\psi\}$, both proposed methods have global convergence to a unique limit point.

V. SIMULATION RESULT

A. Settings

In the following experiments, six University of California Irvine (UCI) regression datasets are used [35]. They are respectively Abalone (ABA) [36], [37], Airfoil Self-Noise (ASN) [38], Boston Housing (HOUSING) [36], [38], Concrete (CON) [39], Energy Efficiency (ENERGY) [38], and Wine Quality (white) (WQW) [40], [41]. For each dataset, its RBF width is selected between 0.1 to 10. The basic setting of each dataset is given by TABLE I.

In the following experiment, the performance of all algorithms is evaluated by the average test set error

$$\bar{\mathcal{E}}_{test} = \frac{P_\beta}{N'} \sum_{i'=1}^{N'} y_{i'}^2 + \frac{1-P_\beta}{N'} \|\mathbf{y}' - \mathbf{A}'\mathbf{w}\|_2^2 + \frac{1-P_\beta}{N'} \mathbf{w}^T \left[(P_\beta + \sigma_b^2) \text{diag}(\mathbf{A}'^T \mathbf{A}') - P_\beta \mathbf{A}'^T \mathbf{A}' \right] \mathbf{w}, \quad (59)$$

where N' denotes the size of test set, $\mathbf{y}' = [y'_1, \dots, y'_{N'}]$, \mathbf{A}' is a $N' \times M$ matrix, and its element in i th row and j th column is

$$[\mathbf{A}']_{i',j} = \exp\left(-\frac{\|\mathbf{x}'_{i'} - \mathbf{c}_j\|_2^2}{s}\right).$$

To better approximate the l_0 -norm term, the first method uses the MCP function with $\gamma = 1.001$. The parameter λ is used to control the number of nodes. The corresponding experimental results are shown in Fig. 2. From Fig. 2, we know that when the value of λ is large, fewer nodes will be used, but the performance of the algorithm will be poor. While the second method introduce a constraint to restrict its number of centers. Unlike the first method, it can directly set the maximal number of centers without introducing any regularization parameter. With different fault scenarios, the corresponding experimental results are given by Fig. 3. From

Dataset	Parameters
ABA	$C = \{0.01, 0.03, 0.06, 0.1, 0.3, 0.6, 1\}$, $\epsilon = \{1, 1.5, 2, 2.5, 3, 3.5, 4, 4.5, 5, 5.5, 6\}$
ASN	$C = \{0.005, 0.01, 0.03, 0.05, 0.1, 0.3, 0.5\}$, $\epsilon = \{0.01, 0.05, 0.1, 0.15, 0.175, 0.2, 0.25, 0.3, 0.35, 0.4\}$
HOUSING	$C = \{0.01, 0.02, 0.04, 0.08, 0.2, 0.4, 0.8\}$, $\epsilon = \{0.01, 0.02, 0.04, 0.08, 0.2, 0.4, 0.8\}$
CON	$C = \{0.01, 0.03, 0.06, 0.1, 0.3, 0.6, 1\}$, $\epsilon = \{0.01, 0.03, 0.06, 0.1, 0.3, 0.6, 1\}$
ENERGY	$C = \{0.005, 0.01, 0.05, 0.1, 0.3, 0.5\}$, $\epsilon = \{0.01, 0.05, 0.1, 0.125, 0.15, 0.2, 0.25, 0.3, 0.35, 0.4\}$
WQW	$C = \{0.001, 0.005, 0.01, 0.05, 0.1, 0.2\}$, $\epsilon = \{0.005, 0.0075, 0.01, 0.025, 0.05, 0.075, 0.1, 0.2\}$

TABLE II: Tuning parameter settings of SVR algorithm.

Fig. 3, we see that if we decrease the number of nodes, the performance of the second method will be worse.

B. Convergence

The convergence of the proposed approaches has been discussed. Here we use the dataset ASN with $\{P_\beta = \sigma_b^2 = 0.01\}$ as an example to intuitively demonstrate their convergence. The results are shown in Fig. 4. From Fig. 4, it is observed that within 100 to 200 iterations both methods converge. If we increase the value of λ in the first method or decrease the number of centers in the second method, these algorithms will converge to a larger objective value. For all other datasets, they have similar properties of convergence.

C. Comparison

In this subsection, we compare our two methods with six other algorithms. They are, respectively, the fault tolerant OLS algorithm (OLS) [21], the fault tolerant l_1 -norm approach (ADMM- l_1) [22], the l_1 -norm regularization approach (l_1 -reg.) [36], the support vector regression algorithm (SVR) [36], the orthogonal forward regression algorithm (OFR) [42] and the Homotopy method (HOM) [43].

The fault tolerant OLS algorithm includes two stages. In the first one, it uses OLS method to generate a sorted list of RBF nodes. In the second stage, it constructs a fault tolerant RBF network with desired number of nodes. The fault tolerant l_1 -norm approach is our previous work. It selects centers and constructs the fault tolerant RBF network simultaneously. But compared with the fault tolerant OLS algorithm, the improvement of the fault tolerant l_1 -norm approach is not very significant.

The l_1 -norm regularization approach [36] also uses the l_1 -norm to control the nodes' number used in the RBF network. But its fault tolerant ability is inadequate. Especially, when the fault level is high.

The SVR algorithm [36] can also train the RBF network and select centers simultaneously. The parameters C and ϵ are used to control the training process. TABLE II shows the parameter settings for different datasets. The SVR algorithm has fault tolerant ability. Since the parameter C is capable to limit the magnitudes of the trained weights. The parameter ϵ is used to control its approximation ability. However, the main drawback of the SVR algorithm is that there is no simple way

Dataset	ADMM-HT		ADMM-MCP		ADMM- l_1		OLS	
	AVG MSE	AVG no. of nodes	AVG MSE	AVG no. of nodes	AVG MSE	AVG no. of nodes	AVG MSE	AVG no. of nodes
ABA	4.579	730.0	4.579	730.2	4.570	726.4	4.641	40.8
ASN	0.01076	412.0	0.01100	409.4	0.01096	401.0	0.00736	401.0
HOUSING	0.00688	136.5	0.00745	135.3	0.00746	134.2	0.00688	129.7
CON	0.00839	337.0	0.00848	327.0	0.0086	351.6	0.0066	203.4
ENERGY	0.00452	325.5	0.00453	328.5	0.00459	324.5	0.00036	324.5
WQW	0.01471	1475.0	0.01473	1490.0	0.01476	1460.0	0.01424	338.0
Dataset	l_1 -reg.		SVR		HOM		OFR	
	AVG MSE	AVG no. of nodes	AVG MSE	AVG no. of nodes	AVG MSE	AVG no. of nodes	AVG MSE	AVG no. of nodes
ABA	4.57	726.4	4.749	777.4	4.592	95.6	5.228	673.7
ASN	0.01096	401.0	0.01020	418.1	0.00667	200.2	0.01275	319.1
HOUSING	0.00746	134.2	0.00782	141.4	0.00567	104.9	0.01248	55.1
CON	0.00860	351.6	0.00719	364.5	0.00632	179.6	0.01329	250.7
ENERGY	0.00459	324.5	0.00340	339.7	0.00290	380.3	0.00549	190.2
WQW	0.01480	1468.0	0.01471	1514.3	0.01417	146.8	0.01505	563.5

TABLE III: Average test MSE over 20 trials under fault-free situation.

Dataset	Fault level	ADMM-HT		ADMM-MCP		ADMM- l_1		OLS	
		AVG MSE	AVG no. of nodes	AVG MSE	AVG no. of nodes	AVG MSE	AVG no. of nodes	AVG MSE	AVG no. of nodes
ABA	$P_\beta = \sigma_b^2 = 0.005$	5.1172	152.0	5.1617	140.9	5.3611	156.2	5.3269	156.2
	$P_\beta = \sigma_b^2 = 0.01$	5.223	198.0	5.2587	174.8	5.5254	202.2	5.4416	202.2
	$P_\beta = \sigma_b^2 = 0.05$	5.6029	353.5	5.6169	313.8	6.2372	356.8	5.8697	356.8
ASN	$P_\beta = \sigma_b^2 = 0.005$	0.01490	150.0	0.01512	142.4	0.01617	154.6	0.01810	154.6
	$P_\beta = \sigma_b^2 = 0.01$	0.01597	204.5	0.01596	193.9	0.01711	209.1	0.01928	209.1
	$P_\beta = \sigma_b^2 = 0.05$	0.01992	341.0	0.02006	323.4	0.02086	347.2	0.02262	347.2
HOUSING	$P_\beta = \sigma_b^2 = 0.005$	0.01511	57.5	0.01527	56.8	0.01583	61.9	0.01654	61.9
	$P_\beta = \sigma_b^2 = 0.01$	0.01643	56.5	0.01656	53.6	0.01743	60.9	0.01832	60.9
	$P_\beta = \sigma_b^2 = 0.05$	0.02129	57.5	0.02135	55.9	0.02343	62.0	0.02476	62.0
CON	$P_\beta = \sigma_b^2 = 0.005$	0.01215	127.5	0.01218	124.2	0.01334	131.5	0.01756	131.5
	$P_\beta = \sigma_b^2 = 0.01$	0.01352	118.5	0.01387	114.7	0.01489	122.6	0.01978	122.6
	$P_\beta = \sigma_b^2 = 0.05$	0.01756	135.0	0.01724	133.1	0.01910	140.0	0.02515	140.0
ENERGY	$P_\beta = \sigma_b^2 = 0.005$	0.00519	157.0	0.00518	150.2	0.00560	161.1	0.00568	161.1
	$P_\beta = \sigma_b^2 = 0.01$	0.00563	162.5	0.00560	156.1	0.00610	167.0	0.00632	167.0
	$P_\beta = \sigma_b^2 = 0.05$	0.00761	229.0	0.00761	222.2	0.00856	233.3	0.00849	233.3
WQW	$P_\beta = \sigma_b^2 = 0.005$	0.01643	110.0	0.01641	106.6	0.01678	119.6	0.01732	119.6
	$P_\beta = \sigma_b^2 = 0.01$	0.01665	160.0	0.01660	142.6	0.01701	169.2	0.01753	169.2
	$P_\beta = \sigma_b^2 = 0.05$	0.01730	373.0	0.01729	355.8	0.01763	385.6	0.01807	385.6
Dataset	Fault level	l_1 -reg.		SVR		HOM		OFR	
		AVG MSE	AVG no. of nodes	AVG MSE	AVG no. of nodes	AVG MSE	AVG no. of nodes	AVG MSE	AVG no. of nodes
ABA	$P_\beta = \sigma_b^2 = 0.005$	5.5938	28.3	5.388	767	51.3834	7.5	580584	3.1
	$P_\beta = \sigma_b^2 = 0.01$	5.9977	25.1	5.5537	748.0	56.2897	5.4	1155290	3.1
	$P_\beta = \sigma_b^2 = 0.05$	8.4599	19.2	6.2801	854.6	62.6329	3.9	5542897	3.1
ASN	$P_\beta = \sigma_b^2 = 0.005$	0.01672	165.2	0.01641	467.2	0.08730	3.3	569.2	2.8
	$P_\beta = \sigma_b^2 = 0.01$	0.02054	57.2	0.01731	609.3	0.09517	3.1	1132.7	2.8
	$P_\beta = \sigma_b^2 = 0.05$	0.03078	20.0	0.02105	621.4	0.11130	3.0	5434.4	2.8
HOUSING	$P_\beta = \sigma_b^2 = 0.005$	0.01798	12.9	0.01716	88.2	0.05489	4.7	3.721	2.4
	$P_\beta = \sigma_b^2 = 0.01$	0.02053	10.6	0.01883	75.5	0.06362	4.0	7.362	2.4
	$P_\beta = \sigma_b^2 = 0.05$	0.02999	6.9	0.02476	87.9	0.07864	3.4	35.160	2.4
CON	$P_\beta = \sigma_b^2 = 0.005$	0.01258	138.5	0.01376	278.5	0.04479	13.1	89.61	4.1
	$P_\beta = \sigma_b^2 = 0.01$	0.01483	94.1	0.01514	271.8	0.05112	11.3	178.25	4.1
	$P_\beta = \sigma_b^2 = 0.05$	0.02358	32.3	0.01942	284.9	0.06605	8.9	855.10	4.1
ENERGY	$P_\beta = \sigma_b^2 = 0.005$	0.00542	155.0	0.00566	293.1	0.02966	26.5	0.05854	9.3
	$P_\beta = \sigma_b^2 = 0.01$	0.00591	159.0	0.00619	363.8	0.03859	21.8	0.06895	8.4
	$P_\beta = \sigma_b^2 = 0.05$	0.01026	123.4	0.00870	211.1	0.06420	14.3	0.10650	4.8
WQW	$P_\beta = \sigma_b^2 = 0.005$	0.01702	39.6	0.01685	1346.1	0.03350	5.2	0.03557	2.2
	$P_\beta = \sigma_b^2 = 0.01$	0.01788	29.6	0.01710	1461.0	0.03970	5.0	1065.9	2.2
	$P_\beta = \sigma_b^2 = 0.05$	0.02419	22.6	0.01811	697.8	0.06621	4.4	5114.1	2.2

TABLE IV: Average test MSE over 20 trials under concurrent faults.

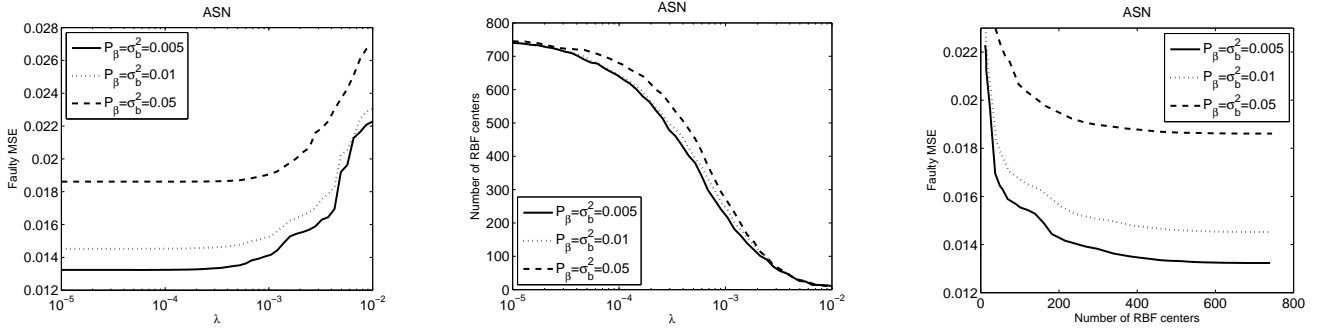


Fig. 2: Properties of ADMM-MCP.

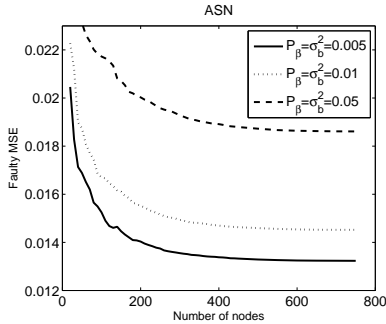


Fig. 3: Properties of ADMM-HT.

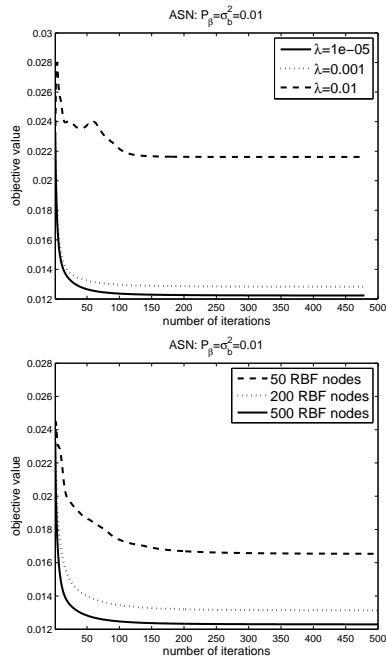


Fig. 4: Convergence of the proposed methods. The first one is the ADMM-MCP method. The second one is the ADMM-HT.

to find an appropriate pair of C and ϵ . In our experiment, we use trial-and-error method to determine them.

The Homotopy method [43] is an incremental learning method. It also uses an l_1 -norm regularization term, and it can tune the regularization parameter automatically. The OFR

algorithm [42] is also an incremental learning method. It chooses one RBF center at a time with the orthogonal forward regression procedure. For OFR, an l_2 -norm regularization term is used. And it can also tune the regularization parameter automatically during training process.

In the following two experiments, the simulation are ran 20 times. And in each trial, the samples of dataset are randomly assigned to the training set and testing set. First, we compare the proposed methods with all above mentioned approaches under the fault-free situation. The typical examples are given by Fig. 5. In this case, the performance of the fault tolerant l_1 -norm approach and the l_1 -norm regularization approach are substantially same with each other. For OLS, HOM, OFR and SVR, we select their minimum MSE and the corresponding number of nodes to represent their performance. For other methods, we use the points where the number of nodes is close to the best result of SVR to represent their performance. It is because that their MSEs are basically decreasing with the increasing of nodes' number.

TABLE III shows the average test set error over the 20 trials. From this table and Fig. 5, it is observed that, under fault-free environment, the performance of OLS and HOM are better than others.

Next, we compare the proposed methods with all other algorithms under concurrent faults. We use three different fault levels: $\{P_\beta = \sigma_b^2 = 0.005\}$, $\{P_\beta = \sigma_b^2 = 0.01\}$ and $\{P_\beta = \sigma_b^2 = 0.05\}$. The typical results of one trial for ASN dataset under different fault levels are given by Fig. 6. Where the first column is the results when $\{P_\beta = \sigma_b^2 = 0.005\}$, while the second column and the third one are respectively the results when $\{P_\beta = \sigma_b^2 = 0.01\}$ and $\{P_\beta = \sigma_b^2 = 0.05\}$. Then, we use the first column as an example to explain these figures. The independent point (694, 0.001538) in the first figure is the best result of SVR algorithm. When we use the similar number of nodes, the results of ADMM-HT, ADMM-MCP, convex ADMM-MCP, ADMM- l_1 and OLS are all similar with each other but better than the SVR method. However, when using fewer centers, such as 150, the performance of the proposed algorithms outperforms others. The second figure in the first column shows the results of HOM and OFR. Both of them break down under concurrent faults. Their minimum test set MSEs are marked in the figure. For other trials and datasets, the results are similar.

In each trial, the best results of SVR, l_1 -reg., HOM, and

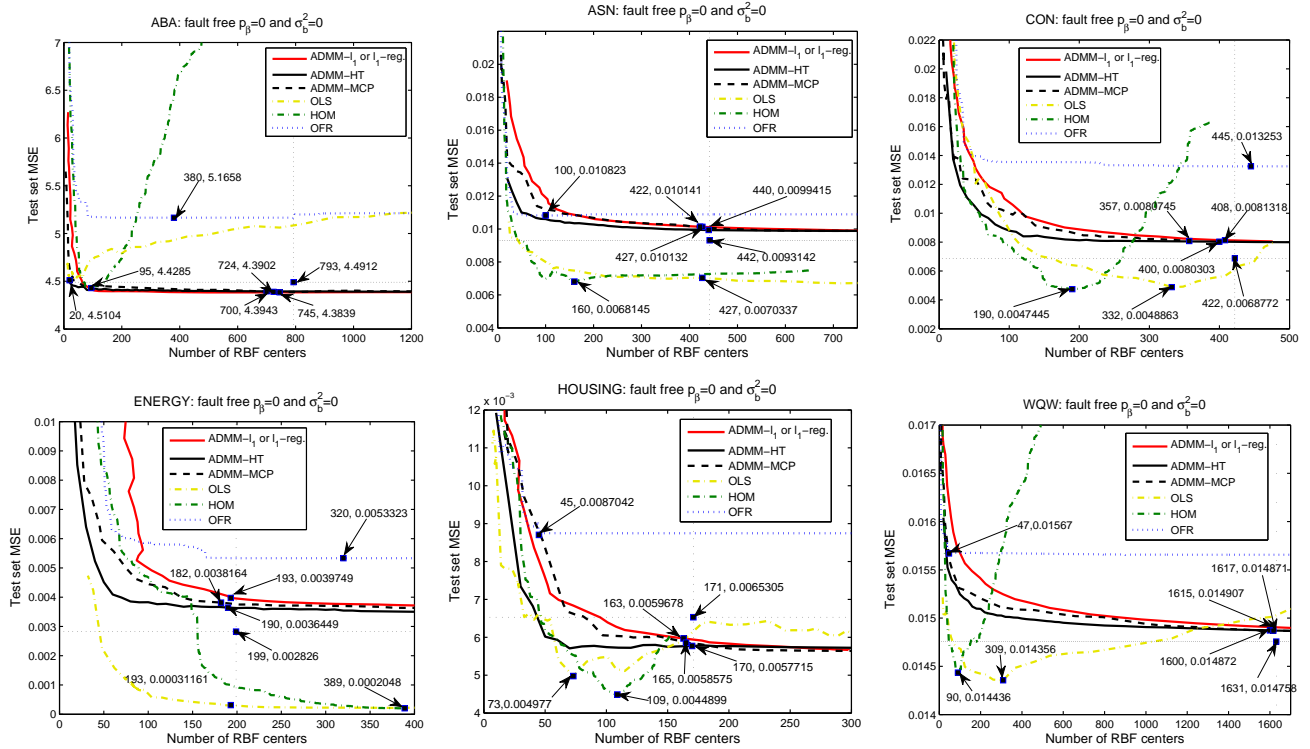


Fig. 5: Performance of different algorithms under fault-free situation.

OFr are selected to represent their performance. For all other algorithms, their MSEs are basically always decreasing with the increasing number of nodes. For ADMM- l_1 , we choose the point with similar performance to the best result of SVR to represent its performance. For ADMM-HT, ADMM-MCP and OLS, the points with similar number of nodes to the selected point of ADMM- l_1 are used. After 20 times trials, we calculate the average test set error and average number of nodes for each algorithm. The results are shown in TABLE IV. From this table, we see that, under the concurrent fault situation, even the best results of SVR, l_1 -reg., HOM, and OFr are used, the performance of them is still unacceptable. However, the ADMM-HT, ADMM-MCP, ADMM- l_1 and OLS can effectively reduce the influence of the concurrent faults. Among them, the ADMM-HT and ADMM-MCP are always the best which have smaller average MSE and use fewer number of nodes. Comparing the proposed two methods, if we carefully tune parameters λ and γ in ADMM-MCP method, it may have better performance than ADMM-HT. But the most attractive thing of ADMM-HT is that we can directly select the number of nodes without tuning any indirect parameter.

Finally, we use the paired t-test to illustrate that compared with existing algorithms the improvement of our proposed algorithms are very significant. From Fig. 6 and TABLE IV, the performance of SVR, l_1 -reg., HOM and OFr are worse than the ADMM- l_1 and OLS method. Hence, we only conduct the paired t-test between the proposed algorithms and ADMM- l_1 and OLS. The results of the t-test are shown in TABLE V and VI. For the one-tailed test with 95% level of confidence and 20 trials, the critical t-value is 1.729. We can see that all

the test t-values are greater than 1.729 and all p-values are smaller than 0.05. In other words, we have enough confidence to say that on average the proposed methods are better than the ADMM- l_1 and the OLS algorithm. Besides, the confidence intervals in TABLE V and TABLE VI do not include zero. Therefore, we can have enough confidence to say that the improvements of our proposed algorithms are very significant.

VI. CONCLUSION

In the paper, the fault tolerant RBF neural network training and its center selection problem are studied. Based on the ADMM framework, two novel algorithms are proposed. They are respectively ADMM-MCP and ADMM-HT. Both of them can handle the two tasks simultaneously. In the first method, the MCP function is introduced to select centers. While, in the second method, an l_0 -norm term is directly used for center selection, and the hard threshold operation is utilized to handle the l_0 -norm term. Both two methods can globally converge to a unique limit point under several mild conditions. From the experimental results, the performance of our proposed approaches are superior to many state-of-the-art methods. The performance of our two algorithms are similar with each other. But ADMM-HT can directly select the number of centers without tuning any regularization parameter.

REFERENCES

- [1] H. Yu, P. Reiner, T. Xie, T. Bartczak, and B. Wilamowski, "An incremental design of radial basis function networks," *IEEE Trans. Neural Netw.*, vol. 25, no. 10, pp. 1793–1803, Oct 2014.
- [2] F. Gianfelici, "RBF-based technique for statistical demodulation of pathological tremor," *IEEE Trans. Neural Netw.*, vol. 24, no. 10, pp. 1565–1574, Oct 2013.

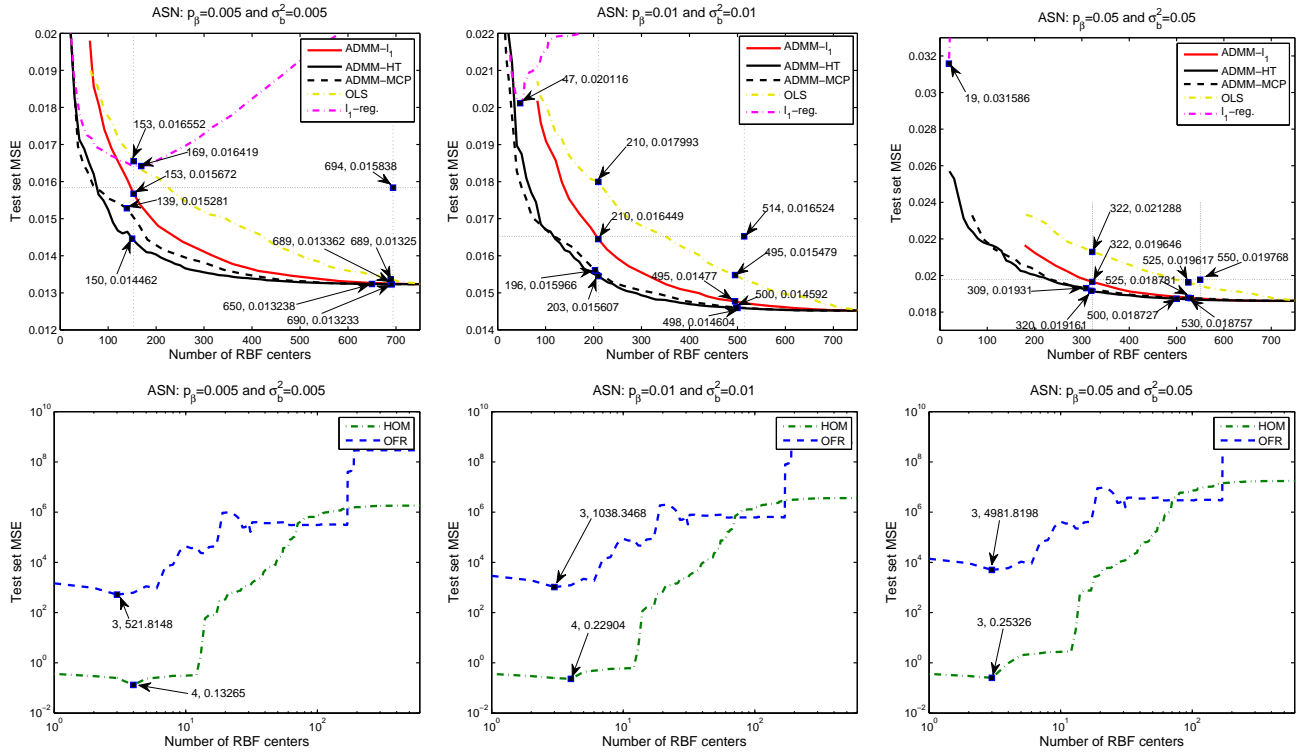


Fig. 6: Performance of different algorithms under concurrent fault situation.

Dataset	Fault level	ADMM-HT v.s. ADMM- l_1					ADMM-MCP v.s. ADMM- l_1				
		AVG diff.	standard deviation	t-value	p-value	Confidence interval	AVG diff.	standard deviation	t-value	p-value	Confidence interval
ABA	0.005	0.244	0.073	15.0	2.75E-12	[0.210,0.278]	0.199	0.065	13.7	1.33E-11	[0.169,0.23]
	0.01	0.302	0.092	14.8	3.66E-12	[0.256,0.349]	0.267	0.092	12.9	3.55E-11	[0.22,0.313]
	0.05	0.634	0.112	25.3	2.14E-16	[0.578,0.691]	0.620	0.111	25.0	2.68E-16	[0.564,0.676]
ASN	0.005	0.00127	0.00030	19.3	2.93E-14	[0.0011,0.0014]	0.00105	0.00033	14.3	6.51E-12	[0.0009,0.0012]
	0.01	0.00114	0.00032	16.1	8.05E-13	[0.0010,0.0013]	0.00115	0.00036	14.5	4.88E-12	[0.0010,0.0013]
	0.05	0.00094	0.00046	9.0	1.30E-08	[0.0007,0.0012]	0.00080	0.00042	8.5	3.29E-08	[0.0006,0.0010]
HOUS-ING	0.005	0.0007	0.00044	7.3	2.99E-07	[0.00051,0.00092]	0.00056	0.00044	5.7	8.50E-06	[0.00035,0.00076]
	0.01	0.0010	0.00053	8.5	3.34E-08	[0.00075,0.00125]	0.00086	0.00050	7.7	1.59E-07	[0.00063,0.00110]
	0.05	0.0021	0.00085	11.3	3.76E-10	[0.00174,0.00253]	0.00208	0.00085	11.0	5.39E-10	[0.00169,0.00248]
CON	0.005	0.00120	0.00042	12.7	4.84E-11	[0.00100,0.00140]	0.00116	0.00041	12.8	4.50E-11	[0.00097,0.00136]
	0.01	0.00137	0.00040	15.3	1.89E-12	[0.00118,0.00156]	0.00102	0.00041	11.0	5.21E-10	[0.00082,0.00121]
	0.05	0.00154	0.00063	11.0	5.40E-10	[0.00125,0.00184]	0.00186	0.00062	13.3	2.23E-11	[0.00156,0.00215]
ENER-GY	0.005	0.00040	0.00023	7.8	1.2E-07	[0.0003,0.000514]	0.00042	0.00023	8.2	6.01E-08	[0.00031,0.00053]
	0.01	0.00047	0.00025	8.3	4.8E-08	[0.00035,0.00059]	0.00050	0.00026	8.7	2.39E-08	[0.00038,0.00062]
	0.05	0.00095	0.00041	10.3	1.6E-09	[0.00076,0.00114]	0.00095	0.00042	10.1	2.12E-09	[0.00076,0.00115]
WQW	0.005	0.00035	0.000128	12.1	1.06E-10	[0.00029,0.00041]	0.00037	0.000130	12.5	6.30E-11	[0.00031,0.00043]
	0.01	0.00036	0.000127	12.6	5.76E-11	[0.0003,0.000415]	0.00041	0.000151	12.1	1.21E-10	[0.00034,0.00048]
	0.05	0.00033	8.66E-05	17.0	2.78E-13	[0.00029,0.00037]	0.00034	0.000107	14.0	9.45E-12	[0.00029,0.00039]

TABLE V: Results of paired t-test between the proposed algorithms and ADMM- l_1 .

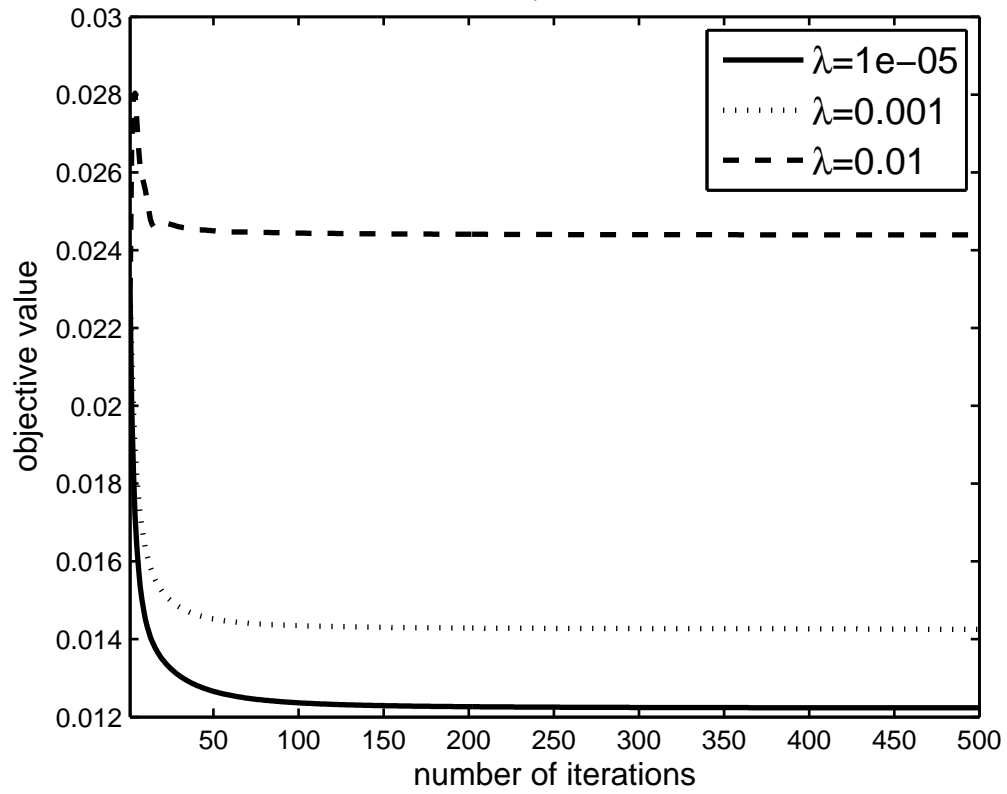
- [3] R. Eickhoff and U. Rückert, "Robustness of radial basis functions," *Neurocomputing*, vol. 70, no. 16, pp. 2758–2767, 2007.
- [4] T. Poggio and F. Girosi, "Networks for approximation and learning," *Proc. IEEE*, vol. 78, no. 9, pp. 1481–1497, 1990.
- [5] S. Haykin, *Neural Networks: A Comprehensive Foundation*, 2nd ed. Upper Saddle River, NJ, USA: Prentice Hall PTR, 1998.
- [6] S. Chen, "Nonlinear time series modelling and prediction using gaussian RBF networks with enhanced clustering and RLS learning," *Electronics Letters*, vol. 31, no. 2, pp. 117–118, 1995.
- [7] S. Chen, C. F. N. Cowan, and P. Grant, "Orthogonal least squares learning algorithm for radial basis function networks," *IEEE Trans. Neural Netw.*, vol. 2, no. 2, pp. 302–309, Mar. 1991.
- [8] J. Gomm and D. Yu, "Selecting radial basis function network centers with recursive orthogonal least squares training," *IEEE Trans. Neural Netw.*, vol. 11, no. 2, pp. 306–314, 2000.
- [9] V. N. Vapnik, *The Nature of Statistical Learning Theory*. New York, NY, USA: Springer-Verlag New York, Inc., 1995.
- [10] A. Smola and V. Vapnik, "Support vector regression machines," *Advances in neural information processing systems*, vol. 9, pp. 155–161, 1997.
- [11] M. Stevenson, R. Winter, and B. Widrow, "Sensitivity of feedforward neural networks to weight errors," *IEEE Trans. on Neural Netw.*, vol. 1, no. 1, pp. 71–80, 1990.
- [12] J. B. Burr, "Digital neural network implementations," in *Neural Networks, Concepts, Applications, and Implementations, Vol III. Englewood Cliffs*. Prentice Hall, 1995, pp. 237–285.
- [13] Z. Han, R.-B. Feng, W. Y. Wan, and C.-S. Leung, "Online training and its convergence for faulty networks with multiplicative weight noise," *Neurocomputing*, vol. 155, pp. 53–61, 2015.
- [14] M. Murakami and N. Honda, "Fault tolerance comparison of ids models with multilayer perceptron and radial basis function networks," in *Proc.*

Dataset	Fault level	ADMM-HT v.s. OLS					ADMM-MCP v.s. OLS				
		AVG diff.	standard deviation	t-value	p-value	Confidence interval	AVG diff.	standard deviation	t-value	p-value	Confidence interval
ABA	0.005	0.210	0.084	11.2	4.05E-10	[0.17,0.249]	0.165	0.0887	8.3	4.54E-08	[0.124,0.207]
	0.01	0.219	0.065	15.0	2.64E-12	[0.186,0.251]	0.183	0.0699	11.7	1.99E-10	[0.148,0.218]
	0.05	0.267	0.048	24.8	3.04E-16	[0.242,0.291]	0.253	0.0487	23.2	1.04E-15	[0.228,0.277]
ASN	0.005	0.00319	0.00099	14.4	5.50E-12	[0.00273,0.00366]	0.00298	0.00104	12.8	4.44E-11	[0.00249,0.00347]
	0.01	0.00331	0.00081	18.3	8.30E-14	[0.00293,0.00368]	0.00368	0.00078	19.0	3.93E-14	[0.00295,0.00368]
	0.05	0.00270	0.00069	17.6	1.66E-13	[0.00237,0.00302]	0.00256	0.00068	16.7	3.97E-13	[0.00224,0.00288]
HOUS-ING	0.005	0.00143	0.00062	10.4	1.37E-09	[0.00114,0.00172]	0.00127	0.00073	7.9	1.12E-07	[0.00093,0.00161]
	0.01	0.00190	0.00071	11.9	1.46E-10	[0.00157,0.00223]	0.00176	0.00072	10.9	6.54E-10	[0.00142,0.00210]
	0.05	0.00347	0.00109	14.2	7.29E-12	[0.00296,0.00399]	0.00340	0.00107	14.2	6.82E-12	[0.00290,0.00392]
CON	0.005	0.00054	0.000429	5.7	9.76E-06	[0.0034,0.0074]	0.00538	0.00430	5.6	1.17E-05	[0.0024,0.0074]
	0.01	0.0063	0.00488	5.7	7.89E-06	[0.0040,0.0085]	0.00590	0.00485	5.4	1.49E-05	[0.0036,0.0082]
	0.05	0.0076	0.00615	5.5	1.25E-05	[0.0047,0.0105]	0.00790	0.00610	5.8	6.70E-06	[0.0051,0.0108]
ENER-GY	0.005	0.00049	0.000229	9.6	5.44E-09	[0.00038,0.00060]	0.00050	0.000227	9.9	3.14E-09	[0.0004,0.0006]
	0.01	0.00069	0.000241	12.9	3.80E-11	[0.00058,0.00081]	0.00072	0.000260	12.3	8.96E-11	[0.0006,0.0009]
	0.05	0.00088	0.000239	16.4	5.40E-13	[0.00077,0.00099]	0.00088	0.000249	15.8	1.06E-12	[0.0008,0.0010]
WQW	0.005	0.00089	0.000290	13.6	1.52E-11	[0.00075,0.00102]	0.00090	0.000286	14.2	7.35E-12	[0.00077,0.00104]
	0.01	0.00088	0.000276	14.3	6.29E-12	[0.00075,0.00101]	0.00093	0.000269	15.5	1.53E-12	[0.00081,0.00106]
	0.05	0.00077	0.000167	20.6	9.04E-15	[0.00069,0.00085]	0.00069	0.000103	30.1	8.50E-18	[0.00064,0.00074]

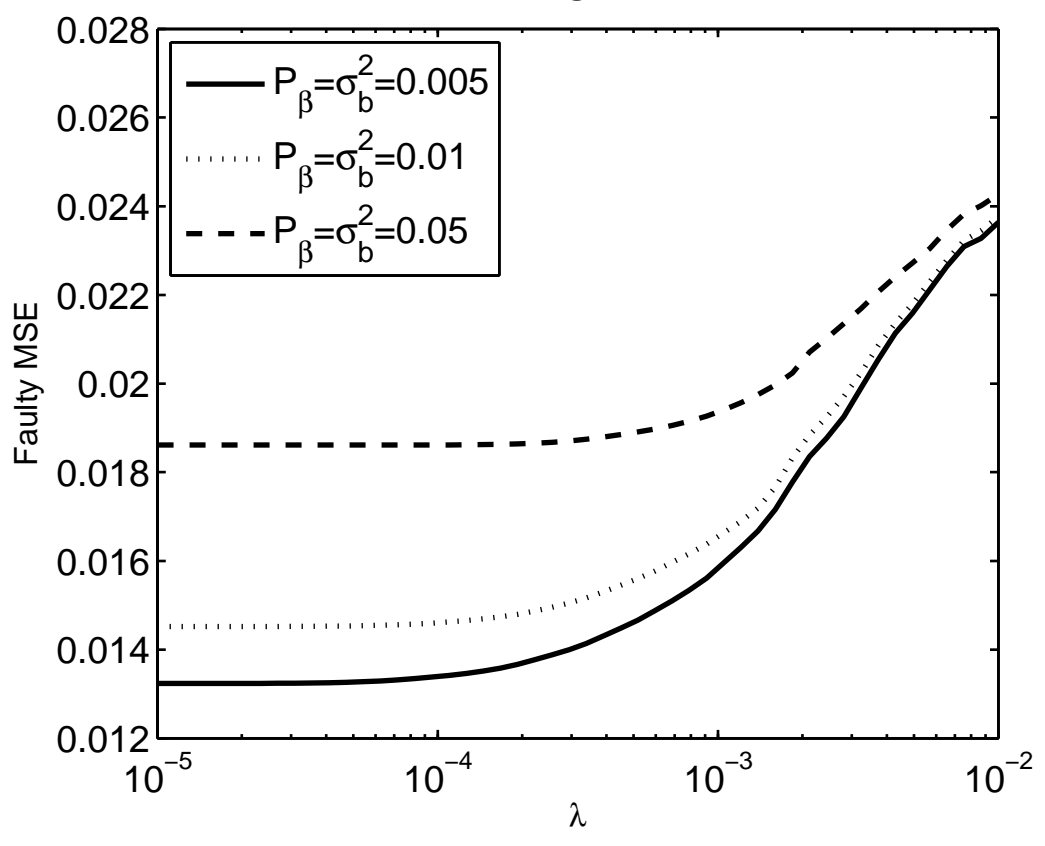
TABLE VI: Results of paired t-test between the proposed algorithms and OLS.

- International Joint Conference on Neural Networks (IJCNN 2007)*, Aug 2007, pp. 1079–1084.
- [15] R. A. Nawrocki and R. M. Voyles, “Artificial neural network performance degradation under network damage: Stuck-at faults,” in *Neural Networks (IJCNN), The 2011 International Joint Conference on*. IEEE, 2011, pp. 442–449.
- [16] J. L. Bernier, J. Ortega, E. Ros, I. Rojas, and A. Prieto, “A quantitative study of fault tolerance, noise immunity, and generalization ability of MLPs,” *Neural Comput.*, vol. 12, no. 12, pp. 2941–2964, 2000.
- [17] C.-S. Leung and J.-F. Sum, “A fault-tolerant regularizer for RBF networks,” *IEEE Trans. on Neural Netw.*, vol. 19, no. 3, pp. 493–507, march 2008.
- [18] M. Conti, S. Orcioni, and C. Turchetti, “Training neural networks to be insensitive to weight random variations,” *Neural Networks*, vol. 13, no. 1, pp. 125–132, 2000.
- [19] M. Lee, K. Hwang, and W. Sung, “Fault tolerance analysis of digital feed-forward deep neural networks,” in *Proc. IEEE International Conference on Acoustics, Speech and Signal Processing (ICASSP2014)*, May 2014, pp. 5031–5035.
- [20] C. S. Leung and J.-F. Sum, “RBF networks under the concurrent fault situation,” *IEEE Trans. Neural Netw. Learn. Syst.*, vol. 23, no. 7, pp. 1148–1155, 2012.
- [21] C.-S. Leung, W. Y. Wan, and R. Feng, “A regularizer approach for rbf networks under the concurrent weight failure situation,” *IEEE Trans. Neural Netw. Learn. Syst.*, vol. 28, no. 6, pp. 1360–1372, 2017.
- [22] H. Wang, R. Feng, Z.-F. Han, and C.-S. Leung, “Admm-based algorithm for training fault tolerant rbf networks and selecting centers,” *IEEE transactions on neural networks and learning systems*, 2017.
- [23] J. B. Burr, “Digital neural network implementations,” *Neural Networks, Concepts, Applications, and Implementations*, vol. III, pp. 237–285, 1991.
- [24] J. Bernier, J. Ortega, I. Rojas, and A. Prieto, “Improving the tolerance of multilayer perceptrons by minimizing the statistical sensitivity to weight deviations,” *Neurocomputing*, vol. 31, pp. 87–103, 2000.
- [25] S. Boyd, N. Parikh, E. Chu, B. Peleato, and J. Eckstein, “Distributed optimization and statistical learning via the alternating direction method of multipliers,” *Found. Trends Mach. Learn.*, vol. 3, no. 1, pp. 1–122, Jan. 2011.
- [26] D. L. Donoho, “Compressed sensing,” *IEEE Transactions on information theory*, vol. 52, no. 4, pp. 1289–1306, 2006.
- [27] C.-H. Zhang *et al.*, “Nearly unbiased variable selection under minimax concave penalty,” *The Annals of statistics*, vol. 38, no. 2, pp. 894–942, 2010.
- [28] P. Breheny and J. Huang, “Coordinate descent algorithms for nonconvex penalized regression, with applications to biological feature selection,” *The annals of applied statistics*, vol. 5, no. 1, p. 232, 2011.
- [29] D. L. Donoho and I. M. Johnstone, “Ideal spatial adaptation by wavelet shrinkage,” *biometrika*, pp. 425–455, 1994.
- [30] Y. Wang, W. Yin, and J. Zeng, “Global convergence of admm in nonconvex nonsmooth optimization,” *arXiv preprint arXiv:1511.06324*, 2015.
- [31] H. Attouch, J. Bolte, and B. F. Svaiter, “Convergence of descent methods for semi-algebraic and tame problems: proximal algorithms, forward-backward splitting, and regularized gauss–seidel methods,” *Mathematical Programming*, vol. 137, no. 1–2, pp. 91–129, 2013.
- [32] R. Baire and A. Denjoy, “Leçons sur les fonctions discontinues: professées au collège de france,” 1905.
- [33] J. Bolte, A. Daniilidis, and A. Lewis, “A nonsmooth morse–sard theorem for subanalytic functions,” *Journal of mathematical analysis and applications*, vol. 321, no. 2, pp. 729–740, 2006.
- [34] S. Zhang, H. Qian, and X. Gong, “An alternating proximal splitting method with global convergence for nonconvex structured sparsity optimization,” in *AAAI*, 2016, pp. 2330–2336.
- [35] M. Lichman, “UCI machine learning repository,” 2013. [Online]. Available: <http://archive.ics.uci.edu/ml>
- [36] Q. Zhang, X. Hu, and B. Zhang, “Comparison of l_1 -norm svr and sparse coding algorithms for linear regression,” *IEEE transactions on neural networks and learning systems*, vol. 26, no. 8, pp. 1828–1833, 2015.
- [37] M. Sugiyama and H. Ogawa, “Optimal design of regularization term and regularization parameter by subspace information criterion,” *Neural Netw.*, vol. 15, no. 3, pp. 349–361, Apr. 2002.
- [38] S. Li, Z.-H. You, H. Guo, X. Luo, and Z.-Q. Zhao, “Inverse-free extreme learning machine with optimal information updating,” *IEEE Transactions on cybernetics*, vol. 46, no. 5, pp. 1229–1241, 2016.
- [39] D. Le Ly and H. Lipson, “Optimal experiment design for coevolutionary active learning,” *IEEE Transactions on Evolutionary Computation*, vol. 18, no. 3, pp. 394–404, 2014.
- [40] R. Ekambara, S. Fefilatye, M. Shreve, K. Kramer, L. O. Hall, D. B. Goldgof, and R. Kasturi, “Active cleaning of label noise,” *Pattern Recognition*, vol. 51, pp. 463–480, 2016.
- [41] P. Cortez, A. Cerdeira, F. Almeida, T. Matos, and J. Reis, “Modeling wine preferences by data mining from physicochemical properties,” *Decision Support Systems*, vol. 47, no. 4, pp. 547–553, 2009.
- [42] X. Hong, S. Chen, J. Gao, and C. J. Harris, “Nonlinear identification using orthogonal forward regression with nested optimal regularization,” *IEEE transactions on cybernetics*, vol. 45, no. 12, pp. 2925–2936, 2015.
- [43] D. M. Malioutov, M. Cetin, and A. S. Willsky, “Homotopy continuation for sparse signal representation,” in *Acoustics, Speech, and Signal Processing. Proceedings.(ICASSP’05). IEEE International Conference on*, vol. 5. IEEE, 2005, pp. 733–736.

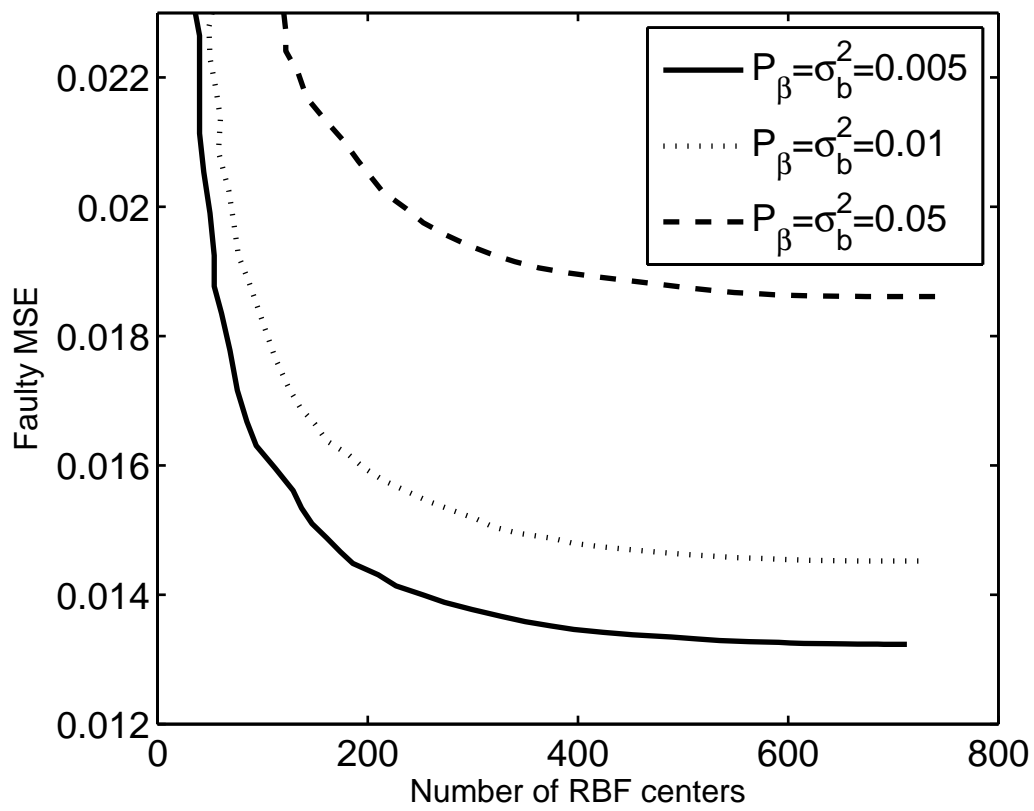
ASN: $P_{\beta} = \sigma_b^2 = 0.01$



ASN



ASN



ASN

